Advances in Estuarine Physics

Article *in* Annual Review of Marine Science · January 2010

DOI: 10.1146/annurev-marine-120308-081015 · Source: PubMed

2 authors, including:

Parker Maccready
University of Washington
95 PUBLICATIONS **4,724** CITATIONS

Advances in Estuarine Physics

Parker MacCready[1] and W. Rockwell Geyer[2]

[1]School of Oceanography, University of Washington, Seattle, Washington 98195-5351; email: parker@ocean.washington.edu

[2]Woods Hole Oceanographic Institution, Woods Hole, Massachusetts 02543; email: rgeyer@whoi.edu

Annu. Rev. Mar. Sci. 2010. 2:35–58

First published online as a Review in Advance on September 15, 2009

The *Annual Review of Marine Science* is online at marine.annualreviews.org

This article's doi: 10.1146/annurev-marine-120308-081015

1941-1405/10/0115-0035$20.00

Key Words

tidally averaged, exchange flow, salt intrusion, stratification, spring-neap

Abstract

Recent advances in our understanding of estuarine circulation and salinity structure are reviewed. We focus on well- and partially mixed systems that are long relative to the tidal excursion. Dynamics of the coupled system of width- and tidally averaged momentum and salt equations are now better understood owing to the development of simple numerical solution techniques. These have led to a greater appreciation of the key role played by the time dependency of the length of the salt intrusion. Improved realism in simplified tidally averaged physics has been driven by simultaneous advances in our understanding of the detailed dynamics within the tidal cycle and across irregular channel cross-sections. The complex interactions of turbulence, stratification, and advection are now understood well enough to motivate a new generation of physically plausible mixing parameterizations for the tidally averaged equations.

1. INTRODUCTION

Estuarine circulation is highly complex, characterized by strong tidal currents, rough bathymetry, energetic turbulence, and steep density gradients born of the competition between ocean and river waters. Despite this complexity, and across enormous variation of these controlling variables, several key characteristics of the tidally averaged circulation and stratification emerge as being common to many systems: Chief among them is the exchange flow. Starting from the classical theoretical framework developed in the mid-twentieth century, we trace the evolution of assumptions and solution approaches for well- and partially mixed systems, focusing on recent advances in the parameterization of tidally averaged turbulent fluxes. These surprisingly simple parameterizations are then scrutinized in light of observational and modeling studies that explore detailed processes within the tidal cycle. Important results are distilled into scaling relations for the tidally averaged stratification, circulation, and salt intrusion. The dominant dynamical role played by the length of the salt intrusion becomes apparent in many studies. However, the time dependency of this length also alters its role in unexpected ways.

This review does not provide a comprehensive treatment of estuarine physics—many important topics have been left out. For example, it does not address the influence of winds and waves, nor that of sediment transport processes. Other reviews (e.g., Fischer 1976, Fischer et al. 1979, Chatwin & Allen 1985, Lewis 1997) provide more comprehensive treatment of dispersion processes. Neither does this review address the dynamics of fjords, lagoons, salt wedges, and other estuarine regimes that lie well outside the partially mixed paradigm. Yet even within this narrow scope, the recent literature is extensive, and the task of reconciling the classic views of estuarine dynamics with modern observations and dynamical interpretations provides an adequate challenge and scope for this review.

2. CLASSICAL TIDALLY AVERAGED BALANCES

The tidally averaged circulation of many estuaries has two extraordinary features. First, despite the net seaward flow due to the river through any cross-section, the deeper half of the water typically flows landward, as shown schematically in **Figure 1*a***. This inflow gradually rises and joins the river flowing outward in the upper half of the estuary, resulting in an overall pattern called the exchange flow. The persistent inflow at depth and associated strong stratification traps particles, larvae, nutrients, and low-oxygen water, giving rise to both the high biological productivity and persistent water-quality problems that characterize estuaries worldwide. Second, the volume flux of the exchange flow is often many times greater than that of the river alone. The corresponding salinity field (**Figure 1*b***) has a gradual along-channel salinity gradient, from oceanic to fresh, because the deep inflowing ocean water is continually freshened by vertical turbulent mixing with the fresher water above. Here, the turbulence is driven by the tides.

A steady balance in which volume is conserved has volume fluxes $Q_1 = Q_2 + Q_R$, with terms defined in **Figure 1**. If salt flux through the mouth is dominated by the exchange flow acting on the tidally averaged salinity, then the net salt balance is

$$V\hat{s}_t = Q_2 s_2 - Q_1 s_1, \tag{1}$$

where V is the volume, $\hat{s}$ is the volume-averaged salinity, and subscript t is the time derivative. Knudsen (1900) showed that in steady state these may be manipulated to give a diagnostic solution for the exchange flow (which is hard to measure) in terms of the stratification at the mouth (which is relatively easy to measure):

$$Q_1 = \frac{s_2}{\Delta s} Q_R, \quad \text{and} \quad Q_2 = \frac{s_1}{\Delta s} Q_R, \tag{2}$$

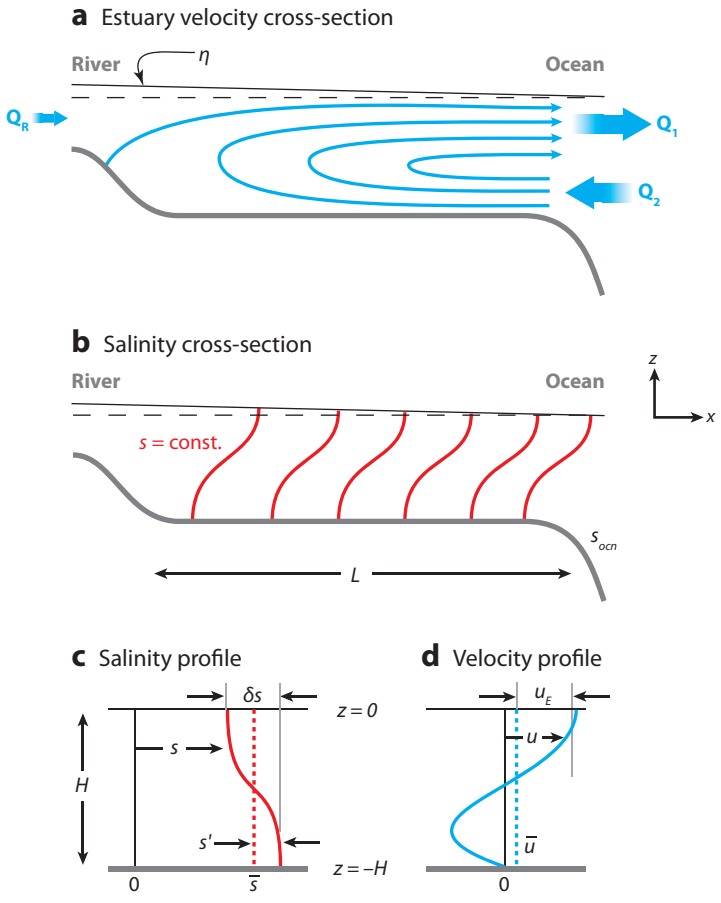

Figure 1

Definition sketch of an idealized partially mixed estuary, showing (*a*) the tidally averaged circulation highlighting the exchange flow and (*b*) isoahalines. Vertical profiles of salinity (*c*) and velocity (*d*) come from the analytical solutions in Equations 8 and 9.

where s_1 and s_2 are the average salinity of out- and inflowing water at the mouth and $\Delta s \equiv s_2 - s_1$ is their difference. For partially mixed estuaries, $\Delta s \approx 1-15$ and $s_2 = s_{ocn} \approx 30-34$, where s_{ocn} is the ocean salinity, implying that the exchange flow is amplified by a factor of 2–34 over the river flow.

The dominant balances in the tidally averaged momentum and salt budgets were first analyzed comprehensively in a remarkable trio of papers by Pritchard (1952, 1954, 1956). Working from extensive salinity and velocity measurements in the James River, a tributary estuary of the Chesapeake, he arrived at the essential balances still used today, which may be written as

$$0 = -\left(1/\rho_0\right) p_x + K_M u_{zz} \quad \text{and} \tag{3}$$

$$s_t + (us)_x + (ws)_z = (K_H s_x)_x + K_S s_{zz}, \tag{4}$$

where u, w, p, and s are the width-averaged, tidally averaged along-channel velocity, vertical velocity, pressure, and salinity, respectively. Subscripts x, z, and t denote partial derivatives. K_M is the vertical eddy viscosity, K_S is the vertical eddy diffusivity. K_H is the along-channel diffusivity

due to tidal correlation of velocity and salinity, rather than turbulent fluxes. Equations 3 and 4 are the approximate result of (*a*) averaging in the cross-channel direction and (*b*) tidal averaging. As written, they assume the simplest possible channel, one with rectangular cross-section of depth H, width B, and sectional area A. Mass conservation is thus expressed as $u_x + w_z = 0$. The system is further simplified by dividing u and s into depth-averaged (overbar) and depth-varying (prime) parts. Thus, $u(x, z, t) = \bar{u}(x, t) + u'(x, z, t)$ with $\overline{u'} = 0$ and similar relations for s. The river flow is given by $\bar{u} = Q_R/A$. In partially mixed systems, the along-channel salinity gradient is dominated by $\bar{s}_x$. Thus, the (hydrostatic) pressure gradient in Equation 3 may be written as $-(1/\rho_0)p_x = -g\eta_x + g\beta\bar{s}_x z$, where η is the free-surface height and the approximate equation of state is $\rho = \rho_0(1 + \beta s)$, with $\beta \cong 7.7 \times 10^{-4}$ psu^{-1}. The equations may then be split into predictive budgets for u', s', and $\bar{s}$:

$$0 = -g\eta_x + g\beta\bar{s}_x z + K_M u'_{zz}, \tag{5}$$

$$u'\bar{s}_x = K_S s'_{zz}, \quad \text{and} \tag{6}$$

$$\bar{s}_t + (\bar{u}\,\bar{s})_x + \left(\overline{u's'}\right)_x = (K_H\bar{s}_x)_x, \tag{7}$$

with details of the derivation given in MacCready (1999, 2004). Equations 5 and 6 assume that the exchange flow and stratification are in quasi-steady balance because they adjust on a timescale comparable to the tidal period. In contrast, $\bar{s}$ adjusts much more slowly, so explicit time dependency must be retained in Equation 7. Given $\bar{s}_x$, Equations 5 and 6 may be solved analytically (Hansen & Rattray 1965), giving rise to polynomial expressions in the dimensionless coordinate $\zeta \equiv z/H$:

$$u = \bar{u}\left(\frac{3}{2} - \frac{3}{2}\zeta^2\right) + u_E\left(1 - 9\zeta^2 - 8\zeta^3\right), \quad \text{and} \tag{8}$$

$$s' = \frac{H^2}{K_S}\bar{s}_x\left[\bar{u}\left(-\frac{7}{120} + \frac{1}{4}\zeta^2 - \frac{1}{8}\zeta^4\right) + u_E\left(-\frac{1}{12} + \frac{1}{2}\zeta^2 - \frac{3}{4}\zeta^4 - \frac{2}{5}\zeta^5\right)\right] \tag{9}$$

(as shown in **Figure 1*c*,*d***). The scale of the exchange flow is given by $u_E = g\beta\bar{s}_x H^3/(48K_M)$. Physically, the pressure gradient due to $\bar{s}_x$ pulls the deep water in, and conservation of mass raises η near the head, forcing surface water out and rapidly enforcing $\bar{u} = Q_R/A$. Bottom and interfacial turbulent stresses bring these accelerations to a steady state: the exchange flow. Then in Equation 6, the exchange flow causes isohalines to slump, increasing s', which is balanced by the tendency of vertical mixing to decrease s'. Thus, both u' and s' depend on $\bar{s}_x$, which in turn reflects the total salt in the estuary. Because $\bar{s} \approx s_{ocn}$ at the mouth and decreases approximately linearly toward the head, any gain in total salt increases the length of the salt intrusion and decreases $\bar{s}_x$. The controlling mechanisms are most clearly understood from an x integral of Equation 7 over the length of the salt intrusion:

$$\underbrace{\frac{d}{dt}\int \bar{s}\,dx}_{\text{STORAGE}} = \underbrace{-\bar{u}\,\bar{s}}_{\text{RIVER}}\ \underbrace{-\left(\overline{u's'}\right)}_{\text{EXCHANGE}} + \underbrace{K_H\bar{s}_x}_{\text{TIDAL}}, \tag{10}$$

where terms on the right-hand side are evaluated near the mouth of the estuary. One term, RIVER, removes salt, whereas EXCHANGE and TIDAL add it. The analytical forms for u' and s' may be used to write EXCHANGE in terms of more fundamental parameters. Then, assuming steady state and $\bar{u} \ll u_E$, one may write Equation 10 to leading order (Hansen & Rattray 1965, Monismith et al. 2002, MacCready 2004) as

$$\underbrace{L_E^3\,\Sigma_x^3}_{\text{EXCHANGE}} + \underbrace{L_H\Sigma_x}_{\text{TIDAL}}\ \underbrace{-\Sigma}_{\text{RIVER}} = 0, \tag{11}$$

where $\Sigma \equiv \bar{s}/s_{ocn}$ and the two length scales are given by

$$L_E = 0.024\left(\frac{c^4}{\bar{u}}\right)^{1/3}\frac{H^2}{\left(K_S K_M^2\right)^{1/3}}, \quad \text{and} \quad L_H = \frac{K_H}{\bar{u}}. \tag{12}$$

The factor $c = \sqrt{g\beta s_{ocn} H}$ is twice the speed of the fastest internal wave that could be supported in the estuary given the density difference between ocean and freshwater. It also corresponds to the maximum outflow velocity that would allow a steady-state salt intrusion based on inviscid theory (Armi & Farmer 1986). In Equation 11, the most basic theory of estuarine salinity structure has thus been reduced to a single first-order ordinary differential equation for $\bar{s}(x)$. However, it is nonlinear, so even for constant coefficients (the length scales), it can be difficult to solve.

Hansen & Rattray (1965) developed the first solution to Equation 11, which has become emblematic of analytic solutions to the coupled equations. The trick they used was to assume that K_H increased linearly toward the mouth as $K_H = K_{H0} + \bar{u}x$ (here defining $x = 0$ at mid-estuary). Then an exact solution is obtained with a perfectly constant value of $\bar{s}_x$ over the central regime (the portion of the estuary away from the head and the mouth). The exchange flow, stratification, and up-estuary salt flux due to EXCHANGE are constant over the central regime in this solution. The ability of RIVER to remove salt increases toward the mouth, proportional to the growing value of $\bar{s}$, and this is balanced by the growing strength of TIDAL. Although this solution has been used extensively, there has been limited theoretical or observational support for the assumed functional form of $K_H(x)$. Chatwin (1976) pursued a different strategy, starting from the assumption that $K_H = 0$. In this case, Equation 11 has an exact solution where $\bar{s}$ varies as $x^{3/2}$. In consequence, $\bar{s}_x$ increases toward the mouth and, with it, the strength of both the exchange flow and the stratification. The increase of exchange flow requires nonzero vertical velocity, which would add a vertical advection term to the approximate Equation 6. However, as long as the bottom to top salinity difference δs is much less than s_{ocn}, the approximations leading to Equation 6 remain valid. The Chatwin solution highlights the formidable leverage exerted by the EXCHANGE term in Equation 11. If $\bar{u}$ doubles, then L_E^3 will be halved, but $\bar{s}_x$ need only increase by $2^{1/3}$. A final possible solution to Equation 11 is for a vertically well-mixed estuary, in which the EXCHANGE flux is negligible. In this case, the solution is $\bar{s} = s_{ocn}\exp(x/L_H)$. These three solutions, along with their characteristic diffusive fraction of up-estuary salt flux (that due to TIDAL), are plotted in **Figure 2*a–c***.

All three analytical solutions place severe limitations on the acceptable mixing coefficients. However, in reality, these are likely to be set by the specifics of tidal currents, bathymetry, and stratification and the variation of these along the channel and in time. Abandoning a fully analytical approach, MacCready (2004) solved Equation 10 numerically, and an example of a more general solution is shown in **Figure 2*d***. In this approach, the mixing coefficients are not constrained a priori, and the solution can readily incorporate variation of B and H along the channel. The numerical framework allows use of more realistic parameterizations of the mixing, as discussed in the next section.

3. MIXING PARAMETERIZATIONS AND SCALING RELATIONS

A complete theory of subtidal estuarine circulation requires knowledge of the mixing coefficients K_M, K_S, and K_H. Ideally, these should be functions of environmental parameters such as bathymetry, river flow, and tides, and they may also be influenced by state variables such as the salinity gradients $\bar{s}_x$ and s'_z. The coefficients are, as a result of tidal averaging, different from familiar eddy diffusivities,

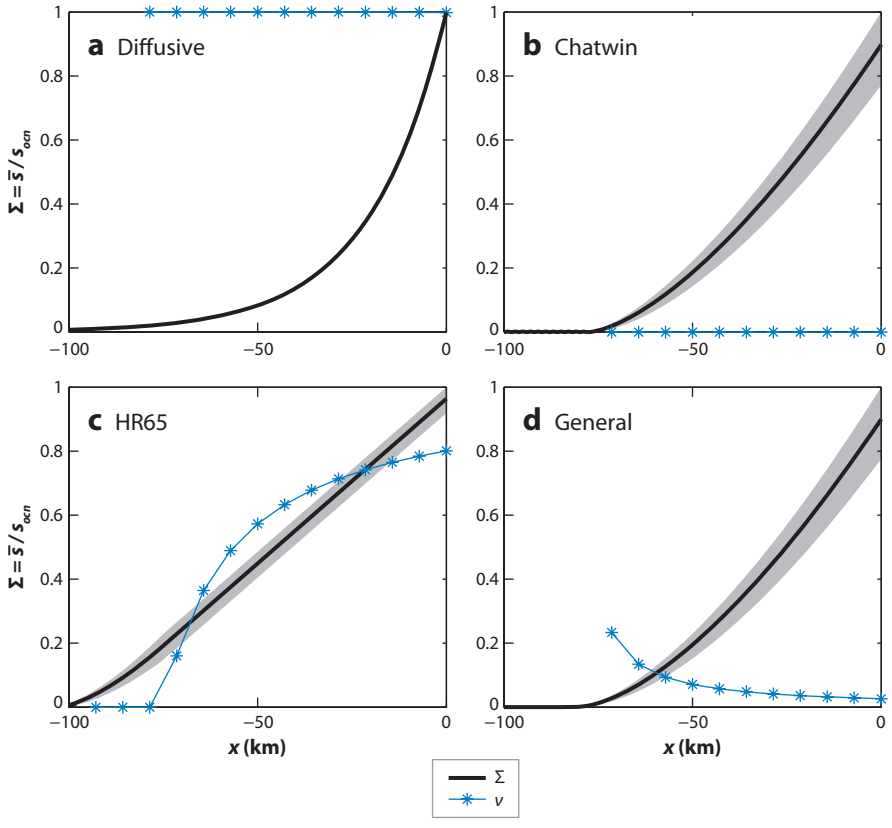

Figure 2

Four steady solutions to Equation 10 with different values of the diffusivities. The normalized section-average salinity, $\Sigma = \bar{s}/s_{ocn}$, is plotted versus x as a thick line, and the gray region around Σ shows the top to bottom range of normalized salinity. The diffusive fraction of up-estuary salt flux ν is also shown. (*a*) Diffusive solution is well mixed, and its up-estuary salt flux is entirely due to TIDAL. (*b*) Chatwin solution has $K_H = 0$ and all the up-estuary salt flux is due to the exchange flow. (*c*) K_H increases in x with gradient $\partial K_H/\partial x = \bar{u}$, reproducing the Hansen & Rattray (1965) central regime solution. (*d*) General solution, with constant K_H. Based on MacCready (2004), reprinted with permission.

and they are better referred to as effective diffusivities, meaning that, when they are multiplied by the appropriate subtidal property gradient, the product gives the correct subtidal flux. For example, defining $\tilde{u}$ and $\tilde{K}_M$ as the tidally varying velocity and eddy viscosity, the effective viscosity is defined as $K_M \equiv \langle \tilde{K}_M \tilde{u}_z \rangle / u_z$, where angle brackets denote tidal averaging.

Early investigators (Hansen & Rattray 1965, Chatwin 1976) determined K_M and K_S empirically, fitting observed profiles of $u'(z)$ and $s'(z)$ to the curves predicted by Equations 8 and 9. Typical values of K_M range from 2 to 100 cm^2 s^{-1}, with K_S equal to approximately half of this. Hansen & Rattray (1966) proposed fundamental relationships between the mixing coefficients and the external parameters, yielding the first truly complete solution for well- and partially mixed estuaries. Recent progress has been driven by observations, particularly those that could be used to infer the effective diffusivities and their parameterization. The detailed interactions of processes within the tidal cycle are discussed in subsequent sections. Here we motivate that discussion by reviewing the basic forms of the resulting parameterizations.

Using extensive measurements of velocity, density, and pressure gradient in the partially mixed Hudson River estuary, Geyer et al. (2000) inferred the tidally varying shear stress and its tidal average. They found that the tidally averaged vertical stress divergence mainly acted to retard up-estuary flow in the lower layer, balancing the pressure gradient arising from $\bar{s}_x$. They also proposed a simple parameterization for the bottom stress based on the tidal average of quadratic drag acting on a tidal current with a small mean flow. Remarkably, without empirical adjustment, this parameterization reproduced the observed estuarine circulation over the 65-day period of their observations. The parameterization may be written as $K_M = a_0 C_D U_T H$, where C_D is a quadratic drag coefficient, U_T is the amplitude of the depth-averaged tidal flow, and a_0 is a numerical constant, discussed further below. Parameterizations of this form are common for channel flow and may physically be interpreted through a mixing-length argument. The breakthrough in Geyer et al. (2000) was its rigorous application to the tidally averaged flow. This simple result appears to work despite its neglect of many processes, notably lateral advection, as discussed in Section 5.

The physics of the effective vertical diffusivity K_S is somewhat different because it relies on mid-depth turbulence rather than the bottom stress. However, exploiting the fact that the mid-depth turbulence is largely forced in the bottom boundary layer, MacCready (2007) proposed a parameterization for K_S of similar functional form to that for K_M, but decreased by a function of the tidally averaged stratification, δs. Again the details of the parameterization arose from observations in the Hudson, this time from extensive microstructure profiles by Peters (1999).

The along-channel diffusivity can result from any correlation of transport and salinity that is not explicitly covered by the RIVER and EXCHANGE terms. A large literature exists on mechanisms of dispersion due to oscillatory flows reviewed by Chatwin & Allen (1985), Fischer et al. (1979), and Zimmerman (1986). These mechanisms can be broadly characterized as either oscillatory shear dispersion (Fischer et al. 1979) or chaotic advection associated with complex trajectories of the spatially variable tidal flow (Zimmerman 1986). Applying Zimmerman's scaling to tidally energetic flow in the complex channel system of Willapa Bay, Banas et al. (2004) quantified K_H using observations of time variation of the net salt and $\bar{s}_x$ at a number of along-channel positions during times of negligible river flow. These were reasonably parameterized as $K_H = 0.035\ U_T B$. Similar to the parameterizations for the effective vertical mixing, this may be interpreted physically as arising from eddies whose velocity is some fraction of U_T and whose length scale is set by channel dimension, in this case the width. MacCready (2004) proposed a modified form of the parameterization above in which the length scale is the smaller of B or the tidal excursion. That paper also proposed a strong increase of K_H within one tidal excursion of the mouth. In general, the parameterization is likely to depend on channel geometry and at this point its value should be considered highly uncertain, pending more observations.

MacCready (2007) incorporated versions of the three mixing parameterizations into a numerical model for the width-averaged, tidally averaged circulation and salinity. The model is configured with along-channel distributions of $H(x)$, $B(x)$, and $U_T(x, t)$ and boundary conditions $Q_R(t)$ and $s_{ocn}(t)$. An example of time-dependent simulation is shown in **Figure 3**. Ralston et al. (2008) extended this model to include wind stress and subtidal sea-level variation, and they applied it to the Hudson River estuary, with extensive comparison to observed velocity and salinity. With some modifications to the vertical-mixing parameterizations, the model skill was comparable to or better than that of a full three-dimensional tide-resolving model (Warner et al. 2005). Although the mixing parameterizations are likely to evolve significantly in the future, we here give the Ralston et al. (2008) versions as our best current guesses and make some dynamical inferences using them. Their parameterizations for K_M and K_S were

$$K_M = a_0 C_D U_T H' \text{ and } K_S = K_M / Sc, \tag{13}$$

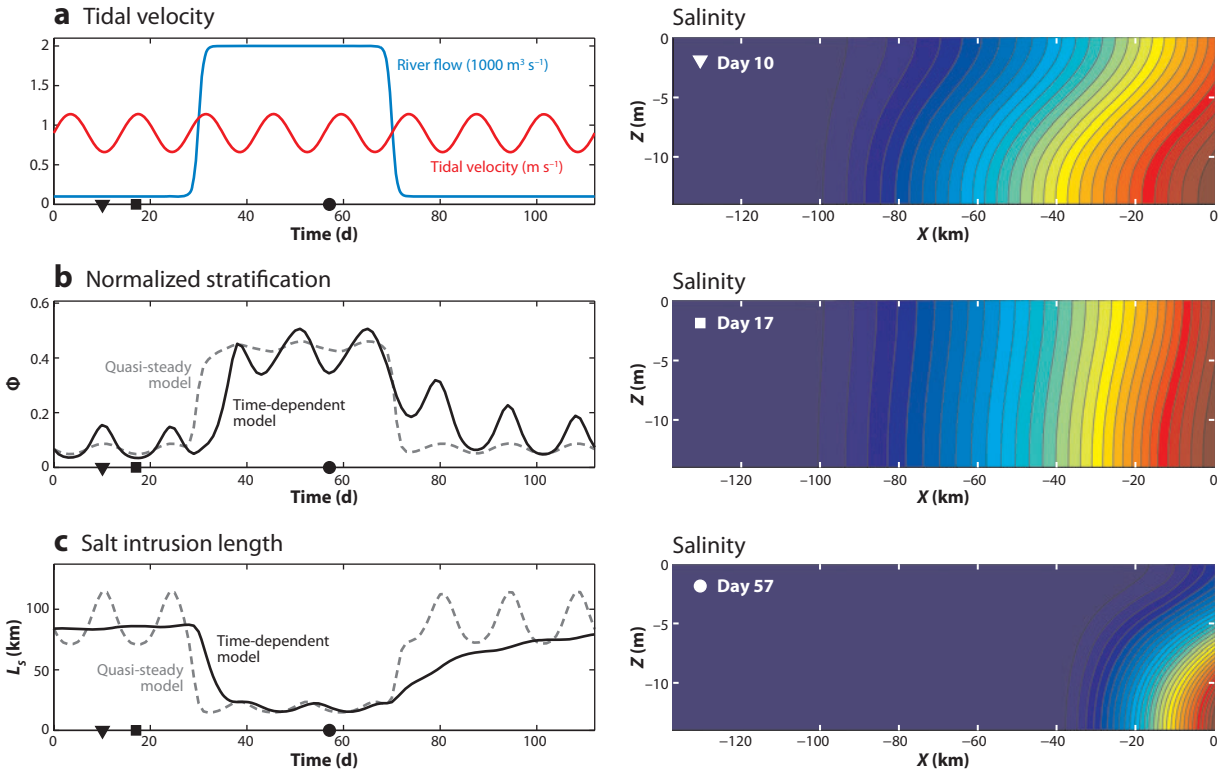

Figure 3

Time-dependent numerical simulation of the Hudson River estuary, showing (*a*) the forcing variation, which consists of a spring-neap cycle of tidal amplitude and a switch from low river flow to high and back again; (*b*) the response of the model stratification versus time, where Φ is the normalized stratification averaged over the length of the salt intrusion; and (*c*) the length of the salt intrusion. To indicate how important unsteady effects might be, the quasi-steady model solution is also plotted (*b*,*c*). Salinity sections at three times are plotted in the right-hand panels, with times shown by symbols in the left-hand panels. These are from low-flow neap, low-flow spring, and high-flow periods. During low-flow periods, the stratification is relatively sensitive to the spring-neap cycle, and the salt intrusion is not, compared with the quasi-steady solution. This is because the salt intrusion does not have time to adjust. Based on MacCready (2007), reprinted with permission.

where $a_0 = 0.028$, $C_D = 2.6 \times 10^{-3}$, and $Sc = 2.2$ is a Schmidt number. They used K_H from MacCready (2007) but this was not a very important parameter. The effect of stratification is included for both K_M and K_S by using H', an estimate of the bottom boundary-layer thickness, given by

$$H' = \min\left(H, H\sqrt{R_{fc}/Ri_x}\right), \tag{14}$$

where $R_{fc} = 0.2$ is the flux Richardson number: the ratio of buoyancy flux to turbulence production. Ri_x is the horizontal Richardson number, a measure of the relative importance of stratification versus mixing, defined and discussed in Section 5.

The forms of the mixing coefficients in Equation 13 from Ralston et al. (2008) are wonderfully simple, and they may be used to demonstrate several important scaling results. For the purposes of this review, we limit our attention to steady-state, exchange-dominated systems where EXCHANGE + RIVER = 0, as in the Chatwin solution. Unsteady effects modify these results

significantly, as described in Section 6. We also assume $\bar{u} \ll u_E$. Then a dimensionless expression for the exchange flow may be written as

$$\frac{u_E}{c} = \frac{1}{48}\frac{cH^2}{K_M}\frac{1}{L}, \tag{15}$$

where we have assumed $\bar{s}_x/s_{ocn} = 1/L$. The dimensionless stratification can similarly be written as

$$\Phi \equiv \frac{\delta s}{s_{ocn}} = \frac{3}{20}u_E\frac{H^2}{K_S}\frac{1}{L}. \tag{16}$$

The final steady-scaling result is for the dimensionless length of the salt intrusion, which may be written as

$$\frac{L}{H} = 0.024\left(\frac{c^4}{\bar{u}}\right)^{1/3}\frac{H}{\left(K_S K_M^2\right)^{1/3}}. \tag{17}$$

A number of important deductions follow directly from these, as discussed, for example, in Hetland & Geyer (2004) with support from idealized numerical simulations. The estuary length is rather sensitive to tidal mixing, varying as K_M^{-1} (and hence as U_T^{-1}). In contrast, the length varies only weakly with river flow, $L \propto \bar{u}^{-1/3}$. But note that in real estuaries the river flow may vary by factors of 10–100, whereas spring-neap variation of tides is more like a factor of 2. Monismith et al. (2002) found $L \propto \bar{u}^{-1/7}$ for the northern San Francisco Bay estuary, attributing the increased stiffness to the effect of stratification on the vertical mixing. Ralston et al. (2008) found that the small exponent could alternatively be explained by along-channel variation of H and B.

The estuarine circulation appears in Equation 15 to vary as K_M^{-1}, and the stratification from Equation 16 would appear to be even more sensitive because it depends on both u_E and K_S^{-1} and hence varies as U_T^{-2}. In fact, the spring-neap variability of the stratification (discussed in Section 6) is the result of this sensitive dependency on tidal flow. However, the dependency on L complicates matters. If L is held fixed, then these inferences are correct. But if L is fully adjusted to the current state of river flow and tides, or, for example, if one is considering very long-term averages or comparing across many different systems, then we may substitute Equation 17 into Equations 15 and 16 to find

$$\frac{u_E}{c} = 0.87Sc^{-1/3}\left(\frac{\bar{u}}{c}\right)^{1/3} \cong \frac{2}{3}\left(\frac{\bar{u}}{c}\right)^{1/3} \quad \text{and} \tag{18}$$

$$\Phi = 5.4Sc^{1/3}\left(\frac{\bar{u}}{c}\right)^{2/3} \cong 7\left(\frac{\bar{u}}{c}\right)^{2/3} \tag{19}$$

using values from the Ralston et al. (2008) parameterizations. These results hold despite the effect of stratification and tidal mixing on H'. The surprise here is that the exchange flow and stratification do not depend on the vertical-mixing coefficients and vary only with the river flow and bathymetry. As described in Park & Kuo (1996) and MacCready (1999), increased mixing (e.g., a step change in time) does initially decrease the exchange flow and stratification. But then the resulting decrease in EXCHANGE causes the estuary to lose net salt, gradually decreasing the length of the salt intrusion. The new steady state arrived at has both higher mixing and shorter L, the two effects exactly balancing as is evident in Equations 18 and 19. Again we must stress that these results apply only to the adjusted (quasi-steady) state, so the adjustment time of L relative to the spring-neap period is of clear importance (Section 6).

A graphical representation of these scaling results is shown in **Figure 4**. The plane $(u_E/c, \Phi)$ represents all possible estuary states. The curve $\Phi\ (u_E/c) = (14/3)(\bar{u}/c)$ is equivalent to the Knudsen relation: The salt lost by the river export is balanced by the gain from the exchange flow. But the Knudsen relation is purely diagnostic: It tells us only which exchange flow is consistent

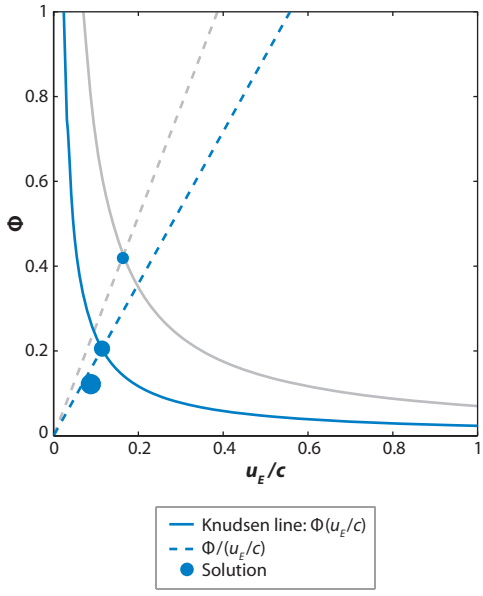

Figure 4

Analytical solution for normalized exchange flow and stratification from Equations 18 and 19. The blue lines are calculated using $c = 2\,\mathrm{m\,s^{-1}}$ and $\bar{u} = 0.01\,\mathrm{m\,s^{-1}}$, and their intersection is the solution for the estuary state (*blue dot*). The larger and smaller blue dots give the solution with tidal mixing increased (*bigger dot*) or decreased (*smaller dot*) by 30%, assuming constant L in Equations 15 and 16. This gives an indication of the possible variation over the spring-neap cycle. The gray lines show the effect of tripling the river flow.

with a given stratification. On its own, it cannot predict both stratification and exchange. The choice of where the solution lies on the Knudsen curve is governed by the details of the mixing, expressed here by the line $\Phi\ (u_E/c)^{-1} = 6.2\ Sc^{2/3}(\bar{u}/c)^{1/3}$. The solution lies at the intersection of these two curves. The length of the salt intrusion would be a third dimension on this state space, one that depends explicitly on the strength of vertical mixing. Also shown in **Figure 4** are unsteady values of the solution point for typical spring and neap variation of the vertical mixing, calculated assuming that L is constant, i.e., completely unadjusted.

4. SPATIAL STRUCTURE OF THE ESTUARINE CIRCULATION

Having discussed above a very simple framework for tidally averaged estuarine structure and mixing parameterizations, we now deconstruct these in light of more detailed views of actual processes.

Fischer (1972) pointed out that the estuarine circulation may not occur in the vertical dimension but rather in the lateral, particularly in wide estuaries. The lateral variation in depth results in a lateral variation in the baroclinic contribution to the vertically integrated pressure gradient, further resulting in down-estuary forcing in the shallow flanks of the estuary and up-estuary forcing in the deep channel. Fischer estimated that the lateral exchange flow is considerably more important than the vertical exchange in the Mersey estuary. Valle-Levinson and colleagues demonstrated the importance (and complexity) of the laterally varying exchange flow in a number of relatively wide estuaries, including the James River (**Figure 5**) (Valle-Levinson et al. 2000) and lower Chesapeake Bay (Valle-Levinson & Atkinson 1999). Wong (1994), Friedrichs & Hamrick (1996), and Kasai et al. (2000) obtained model solutions for the transversely varying estuarine

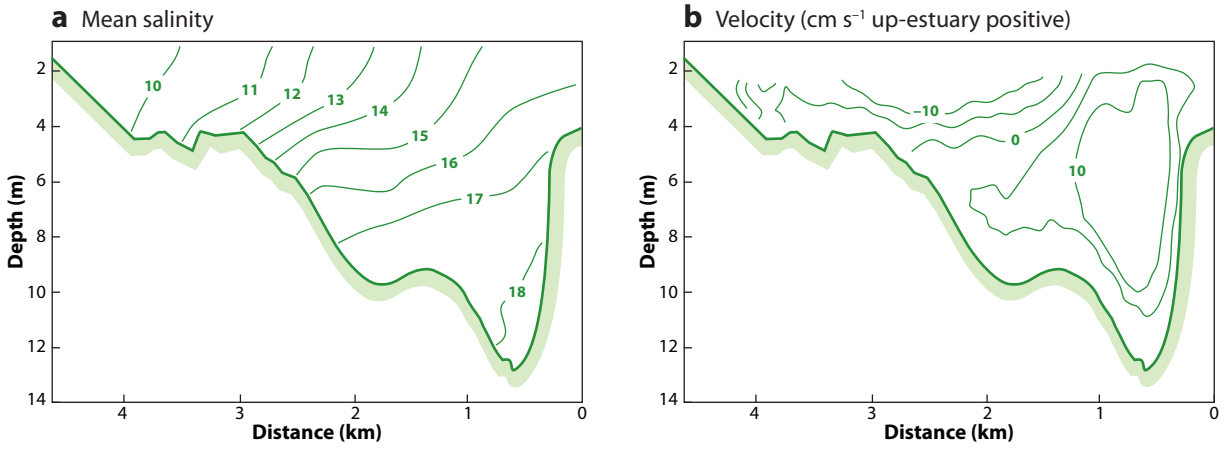

Figure 5

Cross-sections of tidally averaged salinity (*a*) and velocity (*b*) in the James River estuary (looking into the estuary), based on Valle-Levinson et al. (2000). The lateral variations in salinity and velocity are comparable or larger than the vertical variations, so the laterally varying residual circulation is a major contributor to the total salt flux (consistent with the findings of Fischer 1972).

circulation on the basis of the depth-dependent baroclinicity, and their results demonstrated the dominance of lateral rather than vertical variations in the estuarine exchange flow. However, these modeling studies did not consider the influence of the lateral secondary circulation on either the salinity or momentum distribution.

Smith (1976) recognized the important of the lateral (or secondary) circulation as a mechanism for transverse mixing. He showed that the laterally varying along-estuary circulation would induce transverse density gradients—the process now referred to as differential advection (**Figure 6**) (Huzzey & Brubaker 1988, Nunes & Simpson 1985). Smith noted that these gradients would in turn drive lateral motions, which would "mix" the transverse density variations (via transverse shear dispersion). Lacy et al. (2003) suggested that the secondary circulation may also impact the longitudinal momentum structure, and this was confirmed in recent three-dimensional modeling studies by Lerczak & Geyer (2004) and Scully et al. (2009). (The tidal dynamics revealed by these studies are discussed further in Section 5.) These studies indicate that, at least for narrow estuaries, the lateral structure of the estuarine circulation cannot be determined without considering the influence of lateral advection. Lerczak & Geyer (2004) pointed out that the lateral variations are not nearly as strong, and the vertical variations not as weak, as those indicated by the more simplified numerical studies noted in the previous paragraph. Although the lateral structure of the estuarine circulation induced by lateral depth variations can be an important contributor to the overall exchange flow, the secondary flow induced by differential advection maintains a vertical structure similar to the classic estuarine regime described by Pritchard and Hansen and Rattray, at least for relatively narrow estuaries. For wide estuaries and shallow, friction-dominated estuaries, the laterally varying circulation is likely to be more important, although the parameter dependency of this transition has not been fully explored. Valle-Levinson (2008) developed a parameterization to explain the relative importance of width and mixing intensity. However, he did not directly consider the contribution of lateral advection, so his findings need to be verified with a more comprehensive dynamical model.

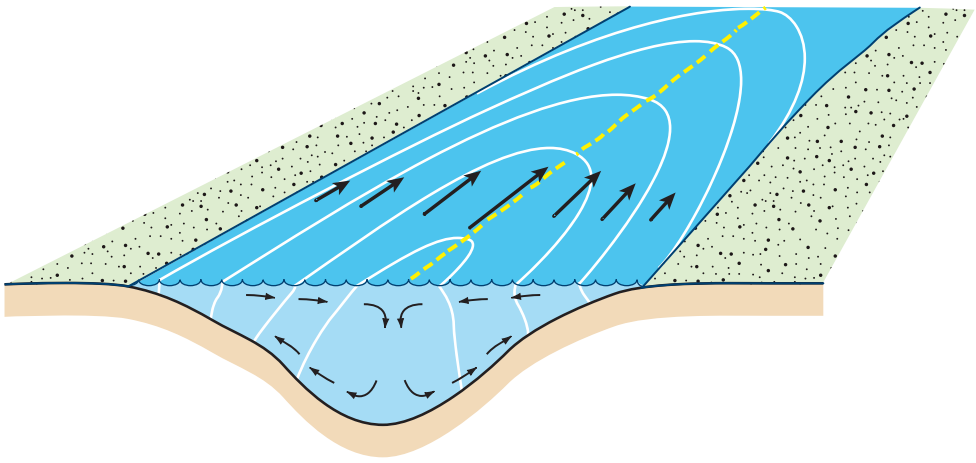

Figure 6

Schematic demonstrating differential advection during flooding tide and its influence on the lateral circulation. Along-estuary velocities (*black arrows*) are stronger in the deep part of the estuary, resulting in greater advection of higher-salinity water (*white contours*) there than on the flanks. The induced lateral density gradient drives a lateral baroclinic circulation with counter-rotating circulation cells. Surface convergence at the center results in the axial convergence front (*yellow dashed line*), as described by Nunes & Simpson (1985).

5. TIDAL EFFECTS ON STRATIFICATION AND RESIDUAL CIRCULATION

In the classic treatment of the estuarine circulation described in Sections 2 and 3, the influence of tides is parameterized in the vertical and horizontal mixing coefficients, and the direct, advective contributions of the tidal motions are removed by the averaging process. Although the averaging of tidal processes provides an effective means of quantifying the density-driven estuarine regime, the tides do more than contribute to turbulence and horizontal dispersion. Tidal shears may significantly affect stratification, and tidal nonlinearities can contribute significantly to the residual circulation. Aided by advances in measurement techniques and numerical models, estuarine researchers have focused much of their attention in recent years on tidal processes and their influence on the stratification and exchange flow.

The term tidal straining was coined by Simpson et al. (1990) to describe the variations of stratification induced by the oscillatory vertical shear of a tidal boundary-layer flow acting on the horizontal salinity gradient (**Figure 7**). Simpson et al. (1990) first applied the idea in explaining the tidal variations of stratification in a portion of Liverpool Bay with a persistent horizontal density gradient. They observed well-mixed conditions during the flooding tide and a return to stratified conditions during the ebb, calling the phenomenon "strain-induced periodic stratification." Tidal straining is a more general term referring to variations in stratification that may not reach the well-mixed limit. Stacey & Ralston (2005) noted that tidal straining occurs only within the vertical extent of the boundary layer, which extends through the water column in weakly stratified estuaries but is capped by the pycnocline in conditions of higher stratification. This is represented in the tidally averaged parameterizations from Equation 13 by the use of H'. Tidal straining usually refers to processes acting in the along-estuary direction, but Lacy et al. (2003) found that straining in the transverse direction may be a more important mechanism in some instances, particularly during spring tides. Their observations indicated that the restratification resulting from lateral straining

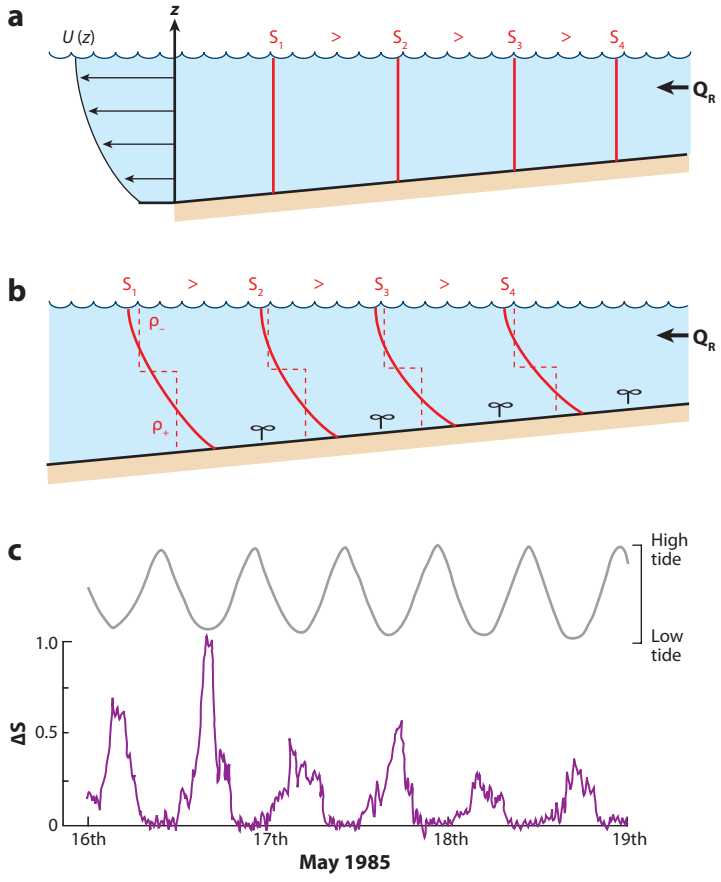

Figure 7

Schematic of the tidal-straining mechanism (*upper panels*) and evidence from Liverpool Bay of the associated tidal periodicity of stratification (*lower panel*) (based on Simpson et al. 1990, reprinted with permission). The top panel illustrates well-mixed conditions at the end of the flooding tide and the vertical profile of ebbing velocity. The solid lines in the second panel show the distortion of the salinity contours by the ebb, and the dashed lines indicate the influence of mixing. The time series in the bottom panel indicates alternation between well-mixed and stratified conditions, with maxima at the end of ebb (low tide).

occurred during the flooding tide, in contrast to the along-estuary straining. The relevance of lateral straining to the spring-neap variation is discussed in Section 6.

Simpson et al. (1990) determined the conditions in which strain-induced periodic stratification should occur on the basis of the balance between tidal mixing and strain-induced restratification. Monismith et al. (1996) and Stacey (1996) simplified Simpson's relation with the introduction of the nondimensional variable $Ri_{x,}$ (the horizontal Richardson number):

$$Ri_x = \frac{\beta g\, s_x\, H^2}{u_*^2}, \tag{20}$$

which indicates the relative importance of baroclinic forcing to bottom stress and where u_* is the friction velocity. Simpson's criterion for strain-induced periodic stratification can be stated simply as $Ri_x < 0.1$. For smaller values of Ri_x, the estuary should remain well mixed through the tidal cycle, and for significantly larger values, it would not reach the well-mixed state at the

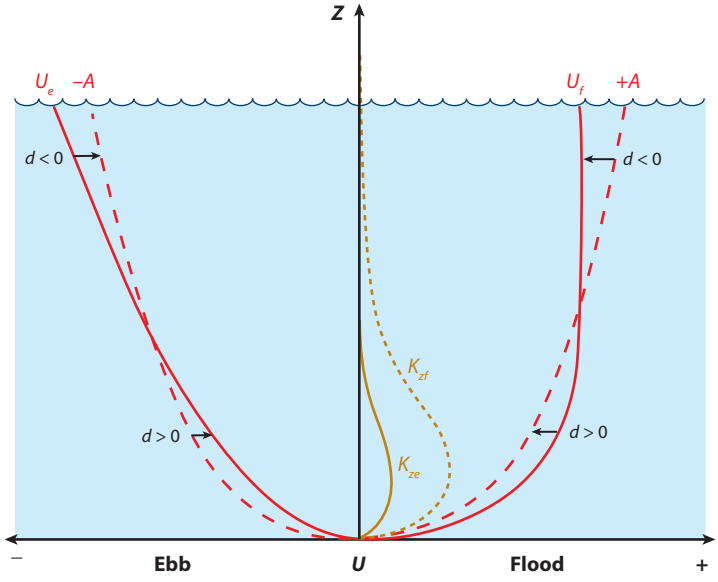

Figure 8

Vertical profiles of velocity and eddy mixing coefficients, demonstrating tidal asymmetry (based on Jay & Musiak 1994). The thick solid lines (U_f and U_e) are the ebb and flood velocity profiles, and the thick dashed lines (−A and +A) indicate the semidiurnal velocity structure. The thin solid and dashed lines are eddy viscosity profiles for flood and ebb, with stronger mixing during the flood. The difference δ between the semidiurnal and actual velocity is the signal of tidal asymmetry. This is made up of a quarterdiurnal component and the mean (landward near the bottom and seaward near the surface.)

end of flood. (More discussion of the threshold of Ri_x is included in the discussion of fortnightly variability, below.) A wide range of Ri_x values have been reported for the occurrence of tidal straining (Stacey et al. 2001, Simpson et al. 1990, Stacey & Ralston 2005, Chant et al. 2007), but there may be some inconsistencies between observations as a result of difficulties in resolving the horizontal salinity gradient at tidal timescales.

One important consequence of tidal straining is its influence on the tidally averaged momentum balance and thus the mean estuarine circulation. Jay & Musiak (1994, 1996) proposed that tidal variability of vertical mixing, which they referred to as tidal asymmetry, can contribute harmonics of the tidal frequency (particularly the M_4 component) and also augment the estuarine circulation. Their observations in the Columbia River of a strong M_4 shear flow, approximately in phase with the flood tide near the bottom and out of phase with the ebb (**Figure 8**), provided the key evidence for the phenomenon. They explained this by the increase of vertical mixing during the flood relative to the ebb due to the strain-induced variations in stratification. Weak or even convectively unstable stratification in the boundary layer during flood allows more vertical mixing, whereas increased stratification during the ebb suppresses mixing. A number of observations have confirmed the tidal variation in mixing intensity due to straining (Stacey et al. 2001, Geyer et al. 2000), and Burchard & Baumert (1998) demonstrated it in a two-dimensional (vertical and along-estuary) numerical model. In addition to the M_4 contribution to vertical shear, tidal asymmetry in mixing contributes to the mean shear in the same sense as the estuarine circulation. The two-dimensional modeling study of Burchard & Baumert (1998) found that the tidal asymmetry in mixing was more important than the baroclinic pressure gradient in contributing to the tidally averaged shear. Note that this presents a grave challenge to the classical view of the estuarine circulation described in Section 2.

Although tidal asymmetry has been given particular emphasis in recent years as a major or even the major contributor to the net estuarine circulation, it is unwise to neglect the direct contribution of the baroclinic pressure gradient. One difficulty with attempts to distinguish linear from nonlinear mechanisms is that both the estuarine circulation and tidal-straining scale with the horizontal Richardson number. Another challenge is that the estuarine circulation contributes to tidal asymmetry by increasing the magnitude of the shear stress and thus the turbulence during the flooding tide (Geyer et al. 2000). Stacey et al. (2001) showed that baroclinically driven exchange flow can occur in a pulselike manner during a short portion of the tidal cycle when vertical mixing is minimal, but its influence is virtually indistinguishable from the time-dependent boundary-layer shear at the turn of the tide. These authors' assessment is that the tidal variability of mixing affects the magnitude and structure of the estuarine circulation, but underlying the rich tidal variability there still remains the fundamental, density-driven flow. This is not to say that the influence of tidal variations of mixing can be neglected, but the neglect of baroclinicity (i.e., the pressure gradient due to $\bar{s}_x$) would be even more egregious.

Another important but only recently recognized contributor to the estuarine circulation is the nonlinear interaction between the lateral (or secondary) circulation and the tidal shear flow. Whereas the mechanism of differential advection is discussed in Section 4 in context with the lateral structure of the estuarine circulation, the influence of the lateral variability on tidal timescales is here discussed. Smith (1976) provided the theoretical treatment of the problem, and Nunes & Simpson (1985) provided compelling observations of the lateral circulations induced by differential advection, in which the longitudinal salinity gradient is rotated into the cross-estuary direction by the transverse shear in the along-estuary flow induced by lateral depth variation. The phenomenon is most commonly manifested during flooding tides, with the faster-moving fluid in the middle of the estuary leading to the advection of denser water in the middle of the estuary and lower-salinity water on the flanks (**Figure 6**). This lateral density gradient drives a baroclinic circulation, with a convergence at the center of the channel that produces the axial convergence front, a phenomenon dramatically demonstrated in the Conwy estuary (Nunes & Simpson 1985). Guymer & West (1991) followed up with a dye study in the Conwy in which they quantified the strength of the lateral circulation. They confirmed the two-cell structure postulated by Smith (1976) and inferred by Nunes & Simpson (1985), and they noted that it was well developed during the flood tide, with stronger lateral gradients.

Although Smith (1976) first identified the importance of the lateral circulation for estuarine kinematics, its influence on dynamics awaited more precise measurements and models. Scott (1994) modeled the lateral circulation induced by differential advection, noting that the along-estuary velocity structure is affected by the transverse circulation. Trowbridge et al. (1999) suggested that lateral advection may explain a mismatch between local bottom stress estimates measured by turbulence-resolving current meters in the Hudson River estuary and integral estimates based on the overall momentum balance. Note that these integral estimates were used by Geyer et al. (2000) to verify the classic estuarine theory, so what Geyer et al. (2000) called "stress" may have been significantly fortified by lateral advection. Lacy et al. (2003) also found that the secondary flow altered the along-estuary momentum balance in their observations in San Francisco Bay.

In an idealized numerical modeling study, Lerczak & Geyer (2004) demonstrated that lateral advection can actually be a dominant driving force for the residual circulation (in the same sense as the density-driven flow). As in earlier studies, they found that the lateral circulation is stronger during flood than ebb, and they explained this asymmetry as the result of the reinforcement of the lateral shear during the flood stage by the advection of low-momentum fluid from the bottom boundary layer to the flanks of the estuary. In addition, the downward advection of momentum in the middle of the channel reduces the vertical shear during the flood. During the reversed

lateral circulation of the ebb, the relatively fast-moving surface current is advected to the flanks, reducing the lateral shear and thus reducing the differential advection of salt, which in turn weakens the transverse circulation. Consequently, the vertical exchange of momentum during the ebb is reduced, allowing stronger shears. Averaged over the tidal cycle, the variations in lateral circulation lead to a net along-estuary circulation in the same sense as the ebb shear, i.e., in the same sense as the estuarine circulation. Thus, the tidal variations of secondary circulation reinforce the estuarine circulation in much the same manner as the tidal asymmetry of mixing described by Jay & Musiak (1994).

Differential advection is only one of several processes contributing to the secondary circulation. Channel curvature, well known in context with the helical flow in rivers (Kalkwijk & Booij 1986, Bathurst et al. 1977), is also important in driving secondary flows in estuaries (Geyer 1993, Seim & Gregg 1997, Chant 2002, Seim et al. 2009). Ekman transport is also an important driving factor, even in small, narrow estuaries, as long as there is adequate stratification to extend the timescale of vertical mixing beyond the inertial timescale (approximately scaled as $u_*/(Hf) < 0.5$) (Kalkwijk & Booij 1986, Winant 2007). Huijts et al. (2009) developed analytical expressions for the influence of all three of these lateral circulation mechanisms on the along-estuary flow. The rectification processes lead to a net up-estuary flow on the right side and down-estuary flow on the left (for an observer looking up the estuary) in the Northern Hemisphere. In application to northern Chesapeake Bay, Huijts et al. (2009) showed that the Coriolis-induced rectification is dominant; in fact, its contribution exceeds that due to the along-channel, baroclinic pressure gradient. Scully et al. (2009) also considered the contributions of the three factors in a numerical study of the Hudson estuary using realistic geometry (**Figure 9**). They also confirmed the importance of the Coriolis-induced rectification term, and they demonstrated the feedback process by which the Coriolis-induced circulation is reinforced during the flood and retarded during the ebb. Interestingly, in these Hudson simulations, the relative contributions of different mechanisms varied throughout the domain, but the net impact was almost always to reinforce the net estuarine circulation.

These recent investigations of nonlinear tidal processes seem to shake the foundations of the classic theory of estuarine circulation. We find ourselves in the paradoxical situation that estuaries appear to behave in a manner consistent with the classical paradigm [as first illustrated by Pritchard and more recently supported by the observations of Geyer et al. (2000) and the success of simple models described in Section 3], yet detailed analyses suggest a prominent and often dominant role of tidal nonlinearities as forcing agents. Scully et al. (2009) demonstrated that some of the nonlinear tidal processes can oppose each other, leading to an apparent linear response to variations in tidal amplitude even though the nonlinear contributors are always important. This question is as yet unresolved. It is clear that the along-channel density gradient is a central player in estuarine dynamics, and it is clear that tidal nonlinearities are also major players in many circumstances. The classical theory has yet to be revised to properly account for the varying contributions of these nonlinearities for different estuarine regimes and to explain fully why the classical theory appears to work so well when nonlineareies are neglected.

6. LOW-FREQUENCY VARIABILITY AND ESTUARINE ADJUSTMENT: SALT INTRUSION, ESTUARINE CIRCULATION, STRATIFICATION

Whereas tidal variability is the most conspicuous and energetic time variation in the estuarine regime, estuaries also vary on longer timescales owing to time dependency of the forcing variables. The two most important sources of variability for the majority of estuaries are the spring-neap modulation of tidal forcing and the variation of freshwater flow, but wind-forcing and sea-level

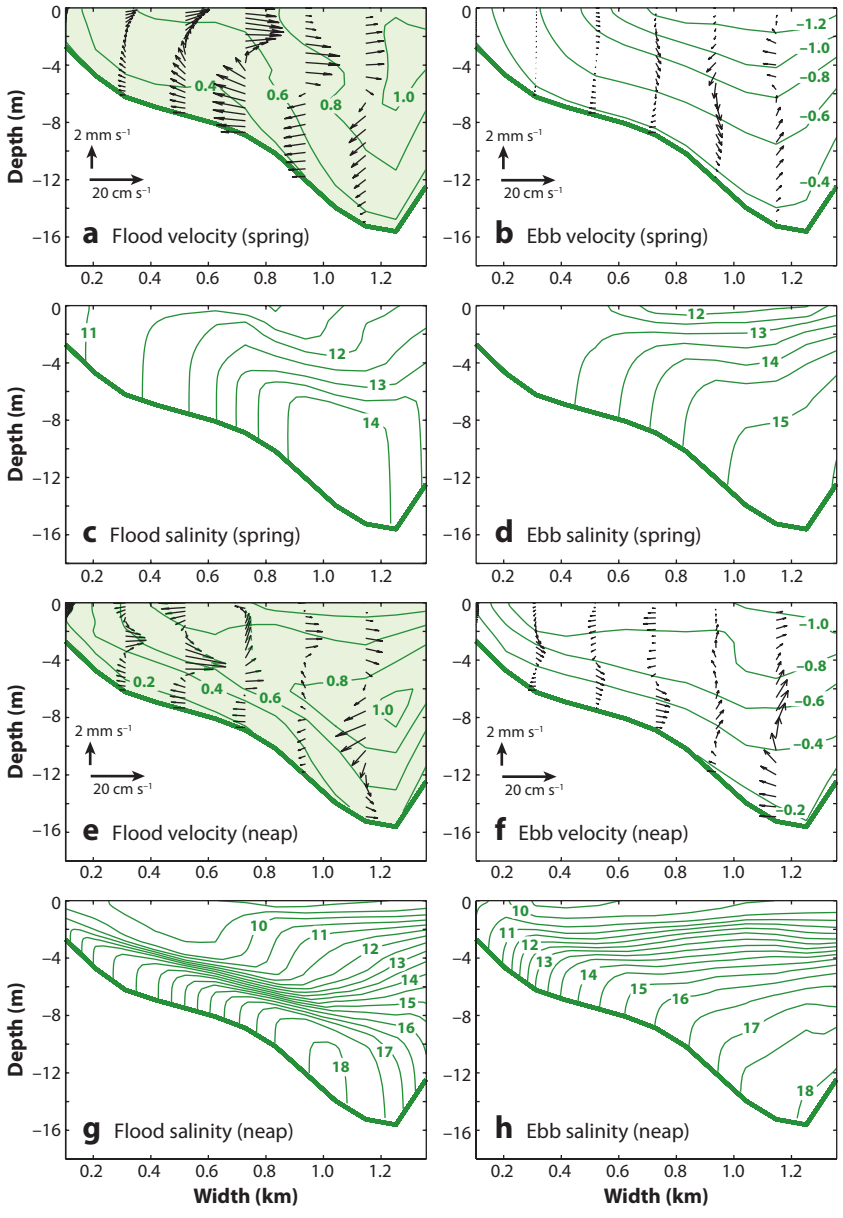

Figure 9

Cross-estuary structure of flood and ebb velocity and salinity during spring and neap tides, based on the realistic-domain numerical model of the Hudson River estuary by Scully et al. (2009). The viewer is looking up the estuary. Along-estuary velocity is shown in contours (m s^{-1}) (*shading indicates flooding tide*), and cross-estuary velocity is shown as arrows. Cross-estuary velocities are significantly higher during floods than ebbs, with a single circulation cell during spring tides and a more complex structure during neaps. Advection by the lateral circulation is an important contributor to the tidally averaged momentum and salt balances, playing a comparable role to vertical mixing.

variations also cause changes in the estuarine regime. These large variations in the estuarine regime indicate that estuaries are not typically in a tidally averaged steady state, but rather in a continual state of adjustment to variations in forcing conditions.

6.1. Response to Varying Tidal Mixing

The spring-neap cycle in estuarine stratification is the most conspicuous and consistent signal of low-frequency estuarine variability. This phenomenon was first documented by Haas (1977) on the basis of a set of observations in subestuaries of Chesapeake Bay, and it is well illustrated by observations in the Hudson estuary (**Figure 10**). The estuaries observed by Haas (1977) as well as the Hudson vary between nearly well-mixed conditions and vertical salinity differences of approximately 10 psu, with the weakest stratification occurring one to two days after spring tides. This variability is not at all surprising, given the fundamental importance of tidal mixing as a controlling variable for estuarine stratification. Perhaps more remarkable is the lack of prior published accounts of this marked variability, which appears to be a ubiquitous occurrence in partially mixed estuaries (Lewis & Lewis 1983, Geyer & Cannon 1982, Stacey et al. 2001).

Closely related to the variation of the stratification is spring-neap variation of the estuarine circulation, which was first reported by Geyer & Cannon (1982). They noted a factor of 2 variation

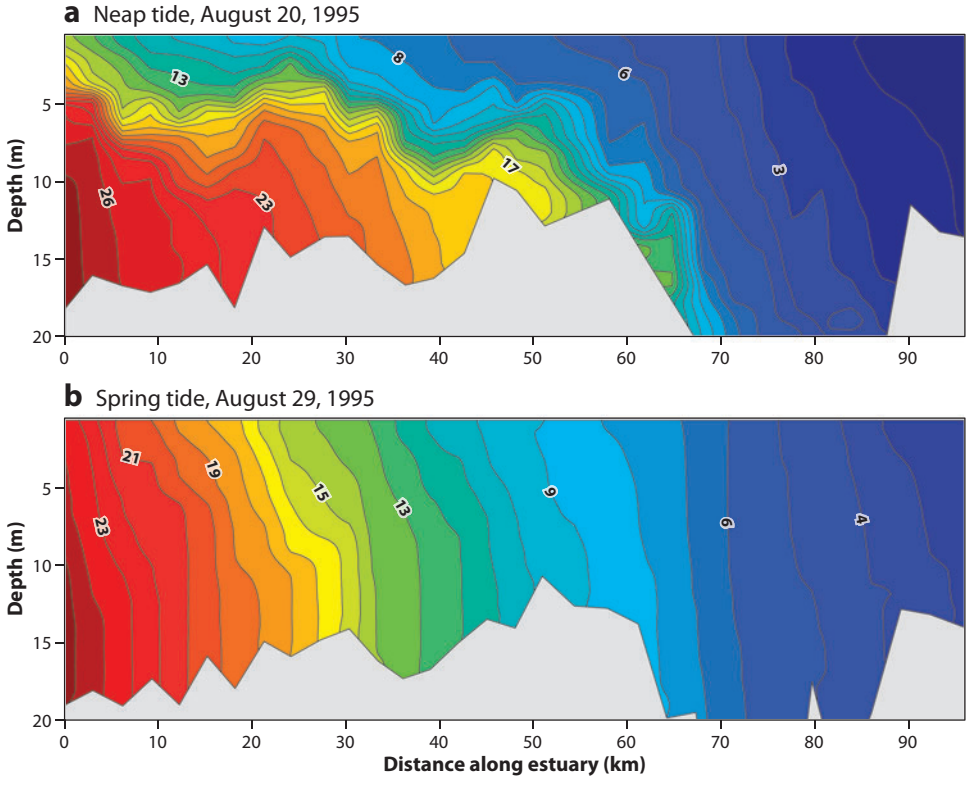

Figure 10

Along-estuary salinity contours in the Hudson River estuary during neap and spring tides, showing the strong spring-neap variation in stratification. The vertically averaged along-estuary salinity distribution changes only slightly, whereas the strength of the stratification changes by an order of magnitude.

in the strength of the exchange flow at the entrance to Puget Sound, with maximum exchange flow occurring during the neaps and minimum during the springs. Geyer and Cannon hypothesized that increased mixing during spring tides results in reduced exchange flow. A number of subsequent researchers have documented spring-neap variations in circulation consistent with the influence of enhanced mixing (e.g., Nunes & Lennon 1987, Monismith et al. 1996, Griffin & LeBlond 1990, Geyer et al. 2000). However, the response of the estuarine circulation to tidal modulation is not as clear as that of the stratification; for example, Lewis & Lewis (1983) found an increase in estuarine circulation during spring tides in the Tees estuary. They attributed this response to tidal rectification due to momentum advection, which could be more important than the modulation of mixing in regions of strong spatial variability (Ianniello 1977, Zimmerman 1986). For relatively simple estuarine geometries, it appears that the variations of mixing are more important than advective nonlinearities, leading to a tendency for stronger exchange flows during neaps than springs.

Attempts to predict the spring-neap transition have been based on the balance between the production of turbulence by the tide-induced shear and the restratification by the estuarine shear flow (Simpson et al. 1990, Stacey et al. 2001, Stacey & Ralston 2005, Chant et al. 2007). The dynamics are closely related to the tidal-straining process, except that the mean shear, rather than the shear of the ebbing tide, is responsible for the restratification. Most recent analyses yield the horizontal Richardson number Ri_x as the governing parameter, although there is considerable variation in the estimate of the threshold value for Ri_x. At the high end, Stacey et al. (2001) indicated a transition to stratified conditions in the northern San Francisco Bay of approximately $Ri_x = 2$; at the low end, Simpson et al. (1990) suggested a transition to well-mixed conditions around 0.1. Individual studies suggest an abrupt transition for any particular estuary, but the critical value may vary. More estimates of Ri_x in different environments are needed to better constrain the threshold value and its dependency on the estuarine geometry.

Motivated by field observations, a number of investigators have simulated the spring-neap transition. Linden & Simpson (1988) performed laboratory experiments with injected bubbles to simulate tidal mixing, demonstrating the variations in both stratification and circulation that occur owing to spring-neap modulation of the tides. Nunes Vaz et al. (1989) used a one-dimensional numerical model to demonstrate the spring-neap variability of stratification due to modulation of tidal mixing. Simpson et al. (1990) also demonstrated spring-neap variations in stratification in their one-dimensional model of the tidal-straining process. Whereas these one-dimensional models effectively illustrate the production of stratification by the residual circulation and its destruction by mixing, these simple simulations exhibit behavior that is not generally observed in real estuaries. One pathological characteristic of one-dimensional simulations is runaway stratification (Monismith et al. 2002, Simpson et al. 1990), resulting from the positive feedback associated with the suppression of turbulence during neap tides. One-dimensional models also tend to show a larger phase lag between minimum mixing and maximum stratification than is observed in estuaries (e.g., Nunes Vaz et al. 1989). Interestingly, three-dimensional modeling results (Warner et al. 2005, Scully et al. 2009) using the same turbulence parameterizations do not exhibit these phase shifts or runaway stratification.

Why the difference in spring-neap transitions between one-dimensional and three-dimensional models? The answer lies in the lateral direction. The along-channel tidal-straining process is not the only mechanism resulting in tidal and spring-neap variations of stratification—lateral straining is another contributor, and it appears to become more important during stronger mixing conditions, according to the aforementioned analysis by Lacy et al. (2003) in San Francisco Bay. Scully et al. (2009) noted that their model simulations exhibit stronger lateral circulations during spring tides (**Figure 9**), and they also noted that stratification is higher during floods

than ebbs, owing to the contribution of lateral straining. Ralston & Stacey (2005) found similar influence of the lateral circulation on restratification during the flood tide in a numerical model of a shallow tidal flat regime. During neap-tide periods of strong stratification, Scully et al. (2009) showed that the lateral circulation provides a mechanism of momentum and salt exchange that compensates for the suppression of turbulence by stratification. Thus, the lateral circulation mitigates the extreme variations in the estuarine stratification that would be produced solely by spring-neap variations in mixing intensity. This explains why the "runaway" regime so conspicuous in one-dimensional models is absent from real estuaries and their three-dimensional simulations.

6.2. Variations in River Flow and Estuarine Length Adjustment

Because the freshwater inflow is an essential forcing agent for the estuarine circulation, it stands to reason that variations of river flow should be an important source of variability. Hansen & Rattray (1965) noted, however, that estuaries tend to have a muted response to changes in river flow, owing to the coupling between momentum, stratification, and salt transport described in Section 3. If the changes in river flow occur over long timescales, then the along-estuary salinity gradient adjusts to a new equilibrium, with a power law

$$L \propto Q_R^{-\alpha}, \tag{21}$$

where α ranges from 1 to one-seventh, with exponents of 1 corresponding to short estuaries dominated by tidal dispersion and values between one-third and one-seventh occurring for partially mixed estuaries as suggested by Equation 12 (Abood 1974, Garvine et al. 1992, Monismith et al. 2002, Bowen & Geyer 2003). Power laws such as Equation 21 have been constructed successfully from data for many estuaries.

Thus, the prevailing view has been one in which estuarine length adjusts to river flow, whereas the stratification and exchange flow adjust to tidal mixing, largely contradicting the steady-state scaling results given at the end of Section 3. The resolution to this contradiction lies in the adjustment time of L. Typically, L adjusts too slowly to change much over the spring-neap cycle, and so the stratification and exchange flow will behave as if L is relatively constant in Equations 15 and 16. In contrast, major variation of the river flow is often seasonal, a timescale over which L can fully adjust for many estuaries, leading to the success of scalings such as Equation 21 (Park & Kuo 1996; Hetland & Geyer 2004; MacCready 1999, 2007).

A theoretical expression for the adjustment time of L was first derived by Kranenburg (1986). By writing the net salt balance Equation 11 in terms of L, and then linearizing around an average value of L, one may show that the adjustment time for L is given by

$$T_{ADJ} = \frac{1}{2}\frac{L}{\bar{u}} \tag{22}$$

for systems dominated by tidal stirring ($L \approx L_H$), and

$$T_{ADJ} = \frac{1}{6}\frac{L}{\bar{u}} \tag{23}$$

for exchange-dominated systems ($L \approx L_E$). These results cover response to variation of river flow, tidal mixing, and ocean salinity (Kranenburg 1986, MacCready 2007). The basic form of the adjustment time in Equation 22 is equivalent to the freshwater replacement time. The reason that the adjustment time is faster in exchange-dominated systems from Equation 23 is that L_E is insensitive to $\bar{u}$ (for adjustment to changes in river flow) or because the EXCHANGE term is very sensitive to U_T (for adjustment to changing tidal mixing).

Consequences of the adjustment time in the case of an idealized model of the Hudson are evident in **Figure 3**. During times of low river flow, $T_{ADJ} \approx 30$ days and L responds little to the spring-neap cycle. At the same time, stratification changes are large, a result of the relative constancy of L.

7. CONCLUSIONS AND FUTURE DIRECTIONS

We consider here just a part of estuarine parameter space: the well- and partially mixed systems typical of drowned river valleys, with a bias toward those whose salt intrusion is long relative to the tidal excursion. Although limited, this description still covers many of the world's important estuaries. Early researchers recognized the importance of tidally averaged properties in such estuaries, particularly the exchange flow and stratification, so they developed equations governing these properties. Progress in understanding this system of equations was relatively slow from the mid- to late-twentieth century because (*a*) the system of equations is fundamentally nonlinear and (*b*) the flux rates due to tidally averaged mixing were very poorly known. Recent advances have been driven by vastly better observations of momentum and salt fluxes within the tide. This has led to a new generation of parameterizations for the tidally averaged mixing. These are still highly simplified, lacking, in particular, any reasonable treatment of the effect of irregular channel shape. In the future, these parameterizations may prove to be a good way of comparing the effects of many competing processes. For example, tidal asymmetry of bottom stress, lateral advection, and Coriolis have all been found to be important, but what relative control do they exert on the exchange flow?

Improved mixing parameterizations have also re-energized the use of width- and tidally averaged equations to explore the complete estuarine system, particularly when applied to numerical solutions of the equations. We have gained a deeper knowledge of how the exchange flow, stratification, and salt-intrusion length are governed by tides and river flow. There has also been improved understanding of the low-frequency variation of these properties due to the spring-neap modulation of tides and changing river flow.

There are many paths suggested here for future research. The effect of irregular channel shape is of clear importance. The many processes grouped into the along-channel effective diffusivity would benefit from extensive observational studies. The connection between tides, mixing, buoyancy flux, and exchange flow may be better made in terms of energy instead of just momentum and salt balances. Finally, the role of low-frequency time dependency is likely to grow in prominence, both for understanding the function of large systems, such as the Baltic, Chesapeake, Long Island Sound, and Puget Sound, and for grappling with the effects of climate change.

DISCLOSURE STATEMENT

The authors are not aware of any biases that might be perceived as affecting the objectivity of this review.

ACKNOWLEDGMENTS

P.M. was supported by NSF grant OCE-0849622. W.R.G. was supported by NSF grant OCE-0824871 and the Mary Sears Chair endowment of the Woods Hole Oceanographic Institution.

LITERATURE CITED

Abood KA. 1974. Circulation in the Hudson River estuary. In *Annals of the New York Academy of Sciences, Hudson River Colloquium*, ed. OA Roels, 250:38–111. New York: NY Acad. Sci.

Armi L, Farmer DM. 1986. Maximal two-layer exchange through a contraction with barotropic net flow. *J. Fluid Mech.* 164:27–51

Banas NS, Hickey BM, MacCready P, Newton JA. 2004. Dynamics of Willapa Bay, Washington, a highly unsteady partially mixed estuary. *J. Phys. Oceanogr.* 34:2413–27

Bathurst JC, Thorne CR, Hey RD. 1977. Direct measurements of secondary currents in river bends. *Nature* 269:504–6

Bowen MM, Geyer WR. 2003. Salt transport and the time-dependent salt balance of a partially stratified estuary. *J. Geophys. Res.* 108(C5):3158; doi:10.1029/2001JC001231

Burchard H, Baumert H. 1998. The formation of estuarine turbidity maxima due to density effects in the salt wedge. A hydrodynamic process study. *J. Phys. Oceanogr.* 28:209–321

Chant R. 2002. Secondary circulation in a region of flow curvature: relationship with tidal forcing and river discharge. *J. Geophys. Res.* 107:3131; doi:10.1029/2001JC001082

Chant RJ, Geyer WR, Houghton R, Hunter E, Lerczak JA. 2007. Bottom boundary layer mixing and the estuarine neap/spring transition. *J. Phys. Oceanogr.* 37:1859–77

Chatwin PC. 1976. Some remarks on the maintenance of the salinity distribution in estuaries. *Estuarine Coast. Mar. Sci.* 4:555–66

Chatwin PC, Allen CM. 1985. Mathematical models of dispersion in rivers and estuaries. *Annu. Rev. Fluid Mech.* 17:119–49

Fischer HB. 1972. Mass transport mechanisms in partially stratified estuaries. *J. Fluid Mech.* 53:671–87

Fischer HB. 1976. Mixing and dispersion in estuaries. *Annu. Rev. Fluid Mech.* 8:107–33

Fischer HB, List EJ, Koh RCY, Imberger J, Brooks NH. 1979. *Mixing in Inland and Coastal Waters*. New York: Academic. 483 pp.

Friedrichs CT, Hamrick JM. 1996. Effects of channel geometry on cross-sectional variation in along channel velocity in partially stratified estuaries. In *Buoyancy Effects on Coastal and Estuarine Dynamics*, ed. DG Aubrey, CT Friedrichs, 53:283–300. Washington, DC: Am. Geophys. Union

Garvine RW, McCarthy RK, Wong K-C. 1992. The axial salinity distribution in the Delaware estuary and its weak response to river discharge. *Estuarine Coast. Shelf Sci.* 35:157–65

Geyer WR. 1993. Three-dimensional tidal flow around headlands. *J. Geophys. Res.* 98:955–66

Geyer WR, Cannon GA. 1982. Sill processes related to deep water renewal in a fjord. *J. Geophys. Res.* 87:7985–96

Geyer WR, Trowbridge JH, Bowen MM. 2000. The dynamics of a partially mixed estuary. *J. Phys. Oceanogr.* 30:2035–48

Griffin DA, LeBlond PH. 1990. Estuary/ocean exchange controlled by spring-neap tidal mixing. *Estuarine Coast. Shelf Sci.* 30:275–97

Guymer I, West JR. 1991. Field studies of the flow structure in a straight reach of the Conwy estuary. *Estuarine Coast. Shelf Sci.* 32:581–96

Haas LW. 1977. The effect of the spring-neap tidal cycle on the vertical salinity structure of the James, York and Rappahannock rivers, Virginia, USA. *Estuarine Coast. Mar. Sci.* 4:485–96

Hansen DV, Rattray M. 1965. Gravitational circulation in straits and estuaries. *J. Mar. Res.* 23:104–22

Hansen DV, Rattray M. 1966. New dimensions in estuary classification. *Limnol. Oceanogr.* 11(3):319–26

Hetland RD, Geyer WR. 2004. An idealized study of the structure of long, partially mixed estuaries. *J. Phys. Oceanogr.* 34:2677–91

Huijts KMH, Schuttelaars HM, de Swart HE, Friedrichs CT. 2009. Analytical study of the transverse distribution of along-channel and transverse residual flows in tidal estuaries. *Cont. Shelf Res.* 29:89–100

Huzzey LM Brubaker JM. 1988. The formation of longitudinal fronts in a coastal plain estuary. *J. Geophys. Res.* 93:1329–34

Ianniello JP. 1977. Tidally induced residual currents in estuaries of constant breadth and depth. *J. Mar. Res.* 35:755–86

Jay DA, Musiak JD. 1994. Particle trapping in estuarine tidal flows. *J. Geophys. Res.* 99:20445–61

Jay DA, Musiak JD. 1996. Internal tidal asymmetry in channel flows: origins and consequences. In *Mixing Processes in Estuaries and Coastal Seas*, ed. C Pattiaratchi, pp. 211–49. Washington, DC: Am. Geophys. Union
Kalkwijk JPT, Booij R. 1986. Adaptation of secondary flow in nearly-horizontal flow. *J. Hydraul. Res.* 24:19–37
Kasai A, Hill AE, Fujiwara T, Simpson JH. 2000. Effect of the Earth's rotation on the circulation in regions of freshwater influence. *J. Geophys. Res.* 105:16961–69
Knudsen M. 1900. Ein hydrographischer Lehrsatz. *Ann. Hydrogr. Mar. Meterol.* 28:316–20
Kranenburg C. 1986. A time scale for long-term salt intrusion in well-mixed estuaries. *J. Phys. Oceanogr.* 16:1329–31
Lacy JR, Stacey MT, Burau JR, Monismith SG. 2003. Interaction of lateral baroclinic forcing and turbulence in an estuary. *J. Geophys. Res.* 108:3089; doi:10.1029/2002JC001392
Lerczak JA, Geyer WR. 2004. Modeling the lateral circulation in straight, stratified estuaries. *J. Phys. Oceanogr.* 34:1410–28
Lewis RE, Lewis JO. 1983. The principal factors contributing to the flux of salt in a narrow, partially stratified estuary. *Estuarine Coast. Mar. Sci.* 16:599–626
Lewis R. 1997. *Dispersion in Estuaries and Coastal Waters*. Chichester, UK: Wiley. 312 pp.
Linden PF, Simpson JE. 1988. Modulated mixing and frontogenesis in shallow seas and estuaries. *Cont. Shelf Res.* 8:1107–27
MacCready P. 1999. Estuarine adjustment to changes in river flow and tidal mixing. *J. Phys. Oceanogr.* 29:708–26
MacCready P. 2004. Toward a unified theory of tidally-averaged estuarine salinity structure. *Estuaries* 27:561–70
MacCready P. 2007. Estuarine adjustment. *J. Phys. Oceanogr.* 27:2133–45
Monismith SG, Burau JR, Stacey MT. 1996. Stratification dynamics and gravitational circulation in northern San Francisco Bay. In *San Francisco Bay: The Ecosystem*, ed. T Hollibaugh, pp. 1–31. Ashland, OR: Pac. Div. AAAS
Monismith SG, Kimmerer W, Burau JR, Stacey MT. 2002. Structure and flow-induced variability of the subtidal salinity field in northern San Francisco Bay. *J. Phys. Oceanogr.* 32:3003–18
Nunes RA, Lennon GW. 1987. Episodic stratification and gravity currents in a marine environment of modulated turbulence. *J. Geophys. Res.* 92:5465–80
Nunes RA, Simpson JH. 1985. Axial convergence in a well-mixed estuary. *Estuarine Coast. Shelf Sci.* 20:637–49
Nunes Vaz RA, Lennon GW, de Silva Samarasinghe JR. 1989. The negative role of turbulence in estuarine mass transport. *Estuarine Coast. Shelf Sci.* 28:361–77
Park K, Kuo AY. 1996. Effect of variation in vertical mixing on residual circulation on narrow, weakly nonlinear estuaries. In *Buoyancy Effects on Coastal and Estuarine Dynamics*, ed. DG Aubrey, CT Friedrichs, pp. 301–17. Washington, DC: Am. Geophys. Union
Peters H. 1999. Spatial and temporal variability of turbulent mixing in an estuary. *J. Mar. Res.* 57:805–45
Pritchard DW. 1952. Salinity distribution and circulation in the Chesapeake Bay estuaries system. *J. Mar. Res.* 11:106–23
Pritchard DW. 1954. A study of the salt balance in a coastal plain estuary. *J. Mar. Res.* 13:133–44
Pritchard DW. 1956. The dynamic structure of a coastal plain estuary. *J. Mar. Res.* 15:33–42
Ralston DK, Stacey MT. 2005. Stratification and turbulence in subtidal channels through intertidal mudflats. *J. Geophys. Res.* 110:C08009; doi:10.1029/2004JC002650
Ralston DK, Geyer WR, Lerczak JA. 2008. Subtidal salinity and velocity in the Hudson River estuary: observations and modeling. *J. Phys. Oceanogr.* 28:753–70
Scott CF. 1994. A numerical study of the interaction of tidal oscillations and nonlinearities in an estuary. *Estuarine Coast. Shelf Sci.* 39:477–96
Scully ME, Geyer WR, Lerczak JA. 2009. The influence of lateral advection on the residual estuarine circulation: a numerical modeling study of the Hudson River estuary. *J. Phys. Oceanogr.* 39:107–24
Seim HE, Gregg MC. 1997. The importance of aspiration and channel curvature in producing strong vertical mixing over a sill. *J. Geophys. Res.* 102:3451–72
Seim HE, Blanton JO, Elston SA. 2009. The effect of secondary circulation on the salt distribution in a sinuous coastal plain estuary: Satilla River GA, USA. *Cont. Shelf Res.* 29:15–28

Simpson JH, Brown J, Matthews J, Allen G. 1990. Tidal straining, density currents, and stirring in the control of estuarine stratification. *Estuaries* 13:125–32

Smith R. 1976. Longitudinal dispersion of a buoyant contaminant in a shallow channel. *J. Fluid Mech.* 78:677–88

Stacey MT. 1996. *Turbulent mixing and residual circulation in a partially stratified estuary*. PhD thesis. Stanford Univ. 209 pp.

Stacey MT, Burau J, Monismith SG. 2001. Creation of residual flows in a partially stratified estuary. *J. Geophys. Res.* 106:17013–37

Stacey MT, Ralston DK. 2005. The scaling and structure of the estuarine bottom boundary layer. *J. Phys. Oceanogr.* 35:55–71

Trowbridge JH, Geyer WR, Bowen MM, Williams AJ. 1999. Near-bottom turbulence measurements in a partially mixed estuary: turbulent energy balance, velocity structure, and along-channel momentum balance. *J. Phys. Oceanogr.* 29:3056–72

Valle-Levinson A, Atkinson LP. 1999. Spatial gradients in the flow over an estuarine channel. *Estuaries* 22:179–93

Valle-Levinson A, Wong K-C, Lwiza KMM. 2000. Fortnightly variability in the transverse dynamics of a coastal plain estuary. *J. Geophys. Res.* 105:3413–24

Valle-Levinson A. 2008. Density-driven exchange flow in terms of the Kelvin and Ekman numbers. *J. Geophys. Res.* 113:C04001; doi:10.1029/2007JC004144

Warner JC, Geyer WR, Lerczak JA. 2005. Numerical modeling of an estuary: a comprehensive skill assessment. *J. Geophys. Res.* 110:C05001; doi:10.1029/2004JC002691

Winant CD. 2007. Three-dimensional tidal flow in an elongated, rotating basin. *J. Phys. Oceanogr.* 37:2345–62

Wong K-C. 1994. On the nature of transverse variability in a coastal plain estuary. *J. Geophys. Res.* 99:14209–22

Zimmerman JTF. 1986. The tidal whirlpool: a review of horizontal dispersion by tidal and residual currents. *Neth. J. Sea Res.* 20:133–54

Annual Review of
Marine Science

Volume 2, 2010

Contents

Errata

An online log of corrections to *Annual Review of Marine Science* articles may be found at http://marine.annualreviews.org/errata.shtml